Electric current and field control of vortex structures in cylindrical magnetic nanowires

Jose A. Fernandez-Roldan,[1,2,*] Rafael P. del Real,[1] Cristina Bran,[1] Manuel Vazquez,[1] and Oksana Chubykalo-Fesenko[1]
[1]*Instituto de Ciencia de Materiales de Madrid, CSIC, 28049 Madrid, Spain*
[2]*Department of Physics, University of Oviedo, 33007 Oviedo, Spain*

(Received 21 April 2020; accepted 17 June 2020; published 15 July 2020)

Magnetization dynamics in a cylindrical Permalloy nanowire under simultaneously applied electric current and field is investigated by means of micromagnetic simulations. The reversal process starts with the creation of open vortex structures with different rotation senses at the nanowire ends. Our results conclude that the current alone enlarges or reduces the size of these vortex structures according to the rotational sense of the associated Oersted field. Large current intensity creates a vortex structure which covers the whole nanowire surface. At the same time the magnetization in the nanowire core remains the same, i.e., no complete magnetization reversal is possible in the absence of external field. The simultaneous action of the current and field allows for the complete control of the vortex structures in terms of setting the polarity and vorticity. The state diagram for the minimum field and current required for the vorticity and axial magnetization switching is presented. This control is essential for future information technologies based on three-dimensional vertical structures, and the presented state diagram will become very useful for future experiments on current-induced domain wall dynamics in cylindrical magnetic nanowires.

DOI: 10.1103/PhysRevB.102.024421

I. INTRODUCTION

Cylindrical magnetic nanowires are considered to be the most promising candidates for the building blocks of three-dimensional (3D) information technologies such as shift registers, magnetic recording, spintronics, logic gates, and sensing architectures [1–9]. Their operation is based on the manipulation of magnetic domains and domain walls which should be controllably nucleated, depinned, and moved along 3D vertical and horizontal tracks.

Cylindrical magnetic nanowires are intrinsically magnetochiral systems. As a result of the cylindrical geometry, magnetic vortex structures are inherent to their magnetism due to the minimization of the magnetostatic energy. They manifest in several situations: as precursors of the magnetization reversal (known as open vortex structures) at the nanowire ends [10], as vortex domains [11,12], and as Bloch domain walls (previously known as vortex domain walls) [13–17]. In all cases the vortices consist of an axially magnetized core (where the magnetization direction defines the polarity of the vortex) and a curling shell (where the azimuthal magnetization component increases with the distance to the axis and its sense of rotation determines the vortex vorticity). The sign of the product of integer numbers (polarity by vorticity) is known as chirality.

The first manifestation of vortices is that demagnetization processes in magnetic nanowires start with curling structures at the nanowire ends with a large axial component and defined chirality. These structures typically exist at the remanence of shape-dominated magnetic nanowires or at the geometrical or compositional constrictions of modulated nanowires and have been observed experimentally [11]. In the ideal case, the initial vortex chiralities are opposite, as set by the demagnetizing field torque (i.e., by the magnetization direction). However, a pattern with the same vortex chiralities at both ends has a very similar energy in long nanowires and is also a viable configuration.

As the field progresses the open vortex structures depin from the nanowire ends/constrictions and may form a propagating Bloch-point domain wall or simply expand along the nanowire, conserving the core magnetization in the same direction and forming a vortex domain. The Bloch-point domain wall is the most typical domain wall in cylindrical magnetic nanowires [10,15–19]. In comparison with planar geometries, cylindrically symmetric Bloch-point domain walls have a vortex structure in the cross-section planes across the nanowire, but they carry a singularity in the middle (where the vortex polarity changes). This singularity, known as the Bloch point, was predicted theoretically and investigated numerically [17,20,21]. The Bloch-point domain walls can be pinned at defects and were recently observed in a static experiment [17]. They are topologically 3D nontrivial structures and are in fact 3D hedgehog Bloch skyrmions [22–24]. They have many appealing properties for applications, e.g., a high mobility under the applied field or current [13,18] and a possibility to achieve very high velocities due to the forecasted absence (or delay) of the internal instabilities known as the Walker breakdown [16,25]. The chirality has been also predicted to affect the domain wall velocity [16,26] due to the magnetic torque effect that promotes the efficient motion of only one type of chirality domain wall. Their nontrivial topology also leads to emerging electromagnetic fields [22].

Finally, the remanent state of nanowires may consist of domains. Axially symmetric vortex domains constitute a

*Corresponding author: jangel.fernandez.roldan@csic.es, fernandezroljose@uniovi.es

generalization of a concept of classical uniform domains in thin films. Vortex-type domains are common for Co-based nanowires with the crystallographic axis perpendicular to their axis. They have been observed by magnetic circular dichroism [11,12] and electron holography [27,28] techniques. As the reversing field progresses, vortex domains can be converted to skyrmion tubes [23,24].

Future technological applications require control of the above vortex configurations. For example, several articles [29–31] suggest the use of multilayered magnetic nanowires as coupled spin-torque oscillators which could use the natural oscillation of the vortex structure in each layer under an applied spin-polarized current as the source of a broadband electromagnetic signal. The question here is to find the minimal conditions where one or another vortex configuration (i.e., vorticity and polarity) can be set. Due to experimental difficulties in studying this because of the variation in many parameters, an initial theoretical study is paramount.

Future applications in information technologies call for spintronics, i.e., manipulation of domain wall dynamics via the application of electrical current, since it holds the promise of energy saving. However, experimental reports on domain wall motion and domain control by means of electric current and thermomagnetic switching in magnetic cylindrical nanowires are very scarce [32,33] and its analysis is very limited [32,34–36]. Particularly, Ref. [32] reports the experimental possibility of changing the vortex (Bloch point) domain wall chirality by means of the Oersted field created by the electric current.

To achieve control over the vortex domains and domain wall dynamics, first it is important to find the conditions for their minimal and efficient manipulation by electric current and field from a theoretical point of view. In this paper we present our modeling results on the manipulation of their vorticity and polarity by the application of external fields and electric current in a Permalloy cylindrical nanowire. Our results show that electric current efficiently manipulates the sense of rotation (i.e., vorticity) of vortex domains via the Oersted field. However, the current alone can only induce domain wall propagation on the nanowire surface without changing its core magnetization which should be assisted by magnetic fields. Importantly, the vorticity and the polarity of the resulting vortex domains do not change simultaneously, so that the control of different patterns is possible by varying the magnitude of the magnetic field and current. We present a diagram for polarity and vorticity switching in terms of the current density and field magnitudes.

II. MODEL

We have modeled the magnetization dynamics of a cylindrical Permalloy nanowire with a diameter $D = 100$ nm using the MUMAX3 micromagnetic code [37]. The simulations always start with the remanent state of the nanowire, obtained from the hysteresis loop with the field applied parallel to the nanowire axis (included in the Supplemental Material [38]). The initial state consists of a uniform axial magnetic domain with open curled structures (precursors of vortex domain walls or domains) with opposite chiralities at each end of the nanowire [see Fig. 1(d)]. A uniform electrical current with density $\mathbf{J}$ and a simultaneous uniform external magnetic field $\mathbf{H}_{\text{ext}}$ are then applied parallel to the nanowire axis. $\mathbf{H}_{\text{ext}}$ is set antiparallel to the magnetization at the initial remanent state.

The magnetization-current interaction is modeled through (i) the Zhang-Li spin transfer torque $\mathbf{T}_{\text{ZL}}$, in the Landau-Lifshitz-Gilbert equation, and (ii) the Oersted magnetic field induced by the electric current. The Zhang-Li torque [39] has the following form,

$$\mathbf{T}_{\text{ZL}} = \frac{1}{1+\alpha^2}\{(1+\xi\alpha)\,\boldsymbol{m}\times[\boldsymbol{m}\times(\boldsymbol{u}\cdot\nabla)\boldsymbol{m}] + (\xi-\alpha)\boldsymbol{m}\times[(\boldsymbol{u}\cdot\nabla)\boldsymbol{m}]\}, \tag{1}$$

where $\boldsymbol{u} = \frac{P\mu_B}{2e\gamma_0 M_S(1+\xi^2)}\boldsymbol{J}$, ξ is the degree of nonadiabaticity, α is the magnetization damping, μ_B is the Bohr magneton, e is the elementary charge, γ_0 is the gyromagnetic ratio, M_S is the saturation magnetization, and P is the electrical current polarization. The Oersted field $\mathbf{H}_{\text{Oersted}}$ induced by the current has been analytically precalculated in an infinitely long straight cylindrical wire. In cylindrical coordinates (r, ϕ, z) the Oersted field is given by

$$\boldsymbol{H}_{\text{Oersted}}\left(r \leqslant \frac{D}{2}\right) = \frac{Jr}{2}\,\boldsymbol{u}_\phi, \tag{2}$$

$$\boldsymbol{H}_{\text{Oersted}}\left(r > \frac{D}{2}\right) = \frac{JD^2}{8r}\boldsymbol{u}_\phi, \tag{3}$$

where $\boldsymbol{u}_\phi$ is the unit azimuthal direction. This magnetic field has only an azimuthal component and reaches a maximum value of $JD/4$ at the nanowire surface (see Supplemental Material [38]).

Micromagnetic simulations have been carried out with the proper parameters for Permalloy, i.e., saturation magnetization $\mu_o M_S = 1$T, exchange stiffness $A_{\text{ex}} = 13\times10^{-12}\,\text{J m}^{-1}$, damping constant $\alpha = 0.02$, nonadiabaticity of the spin-transfer torque parameter $\xi = 0.1$, and the electrical current polarization $P = 0.56$ [37]. Discretization sizes $\leqslant$2.5 nm have been set. The value of the uniform external field H_{ext} was considered between 100 and 500 Oe, and the current density magnitude J up to a maximum value of 10^{12}A m^{-2}.

III. RESULTS

The resulting stationary magnetic configurations under applied current and no external magnetic field are summarized in Fig. 1. For low current densities ($|J| \leqslant 6\times10^{11}\,\text{A m}^{-2}$), the axial magnetization of the remanent state in Fig. 1(d) is not largely affected. However, in a fraction of the first nanosecond almost the whole nanowire acquires some azimuthal magnetization component in the shell with an orientation in the Oersted field direction, as can be observed in the middle cross section in Figs. 1(c) and 1(e) (and in the dynamic calculations presented in the Supplemental Material [38]). This results in the expansion of that vortex structure from the end of the nanowire which has the same chirality as the Oersted field, and the contraction of the one with opposite chirality. The latter can be viewed as the propagation of the vortex on the surface without changing the inner magnetization (i.e., the

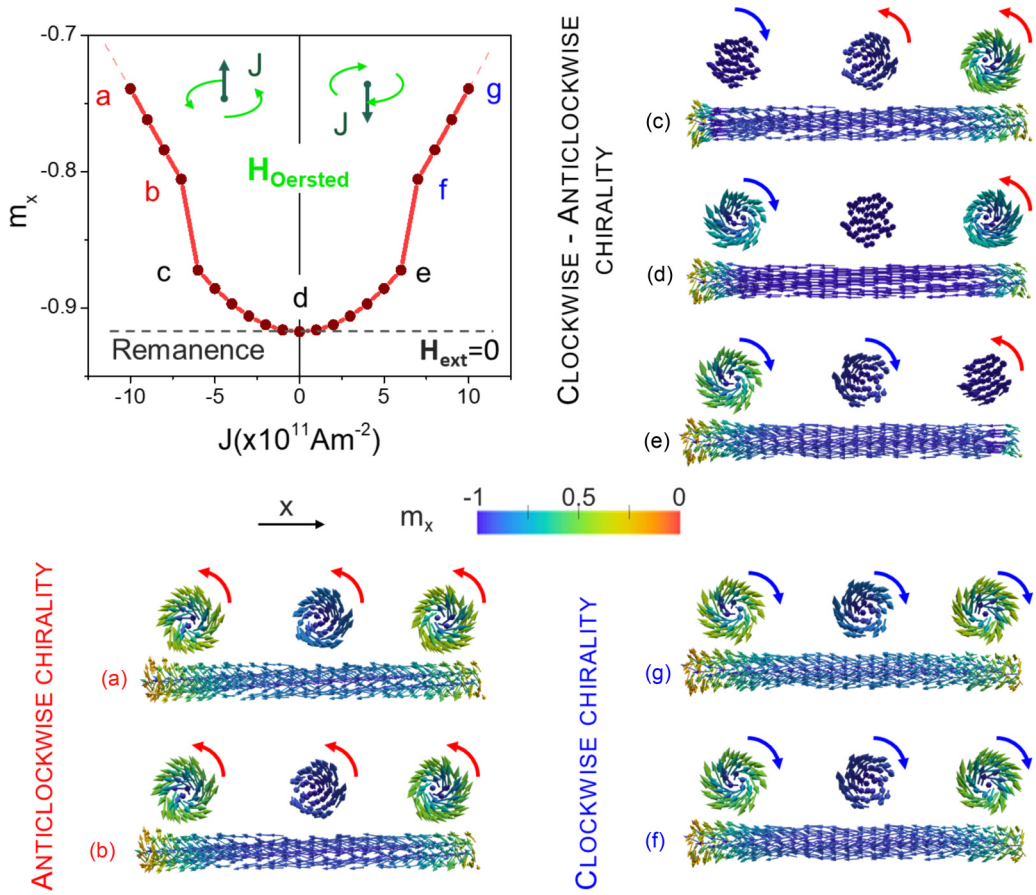

FIG. 1. Top left panel: The axial magnetization component of the stationary state as a function of the current density for $H_{\text{ext}} = 0$. (a)–(e) Magnetization configurations for the applied current values indicated labels in the graph. The configurations (c)–(e) correspond to the situation where no chirality switching has been observed. In the configurations (a) and (b) the resulting chirality is anticlockwise, while for the configurations (f) and (g) the chirality has been switched to clockwise, defined by the Oersted field azimuthal direction.

vortex polarity). The vortex structure with an opposite rotation sense almost disappears for $|J| \geqslant 6 \times 10^{11}\,\text{A m}^{-2}$.

For high current densities ($|J| > 6 \times 10^{11}\,\text{A m}^{-2}$), the absolute value of the axial magnetization is largely decreased, compared with the values obtained for lower current densities (see Fig. 1 Top left panel). Again, the nanowire magnetization first acquires a curling on the surface in the Oersted field direction in the first fractions of a nanosecond. After that there is a subsequent switching of the rotation sense of the vortex structure which initially had opposite chirality to the Oersted field (see Supplemental Material [38]). The switching is followed by the propagation of both vortex domains (with no change in the core magnetization direction) from the ends of the nanowire towards its center, together with a release of the energy by spin-wave emission. The stationary state consists of an almost axial domain with magnetization curling in the shell promoted by the Oersted field, with stronger curling at the nanowire ends corresponding to open vortex structures with the same vorticity. Importantly, the whole process is accomplished in a timescale below 2 ns. The change in the current direction J sets the chirality in the opposite direction.

The evaluation of the length of each vortex domain as a function of the applied current is presented in Fig. 2 (left) (see Supplemental Material for further details [38]). At remanence ($J = 0$), both vortices are confined in the first 220 nm near the ends of the nanowire [see Fig. 2 (right)]. For a small current ($1 \times 10^{11}\,\text{A m}^{-2}$), the vortex domain with the same chirality as the Oersted field extends up to 330 nm, while the other one squeezes to 170 nm. For higher currents the difference in vortex domain lengths becomes more dramatic, and if $J > 6 \times 10^{11}\,\text{A m}^{-2}$, the squeezed vortex is annihilated, leaving a unique vortex structure along the nanowire length as observed in Fig. 2. It is worth noticing that the width of the axially magnetized core of the vortex is not homogeneous along the nanowire length and is wider in positions closer to the nanowire center (far from the nanowire ends). This behavior is only observed for currents larger than $J > 1 \times 10^{11}\,\text{A m}^{-2}$.

The above results indicate that under the action of the current alone it is possible to switch the vortex structure chirality towards the direction of the Oersted field and propagate the vortex structure on the nanowire surface. However, no change in the nanowire core magnetization direction, i.e., complete magnetization switching, seems to be possible.

It is natural to help the magnetization switching with an axially applied magnetic field (pointing opposite to the axial magnetic domain), applied simultaneously with the current. The results are presented in Fig. 3(a) showing the axial magnetization component as a function of the applied field

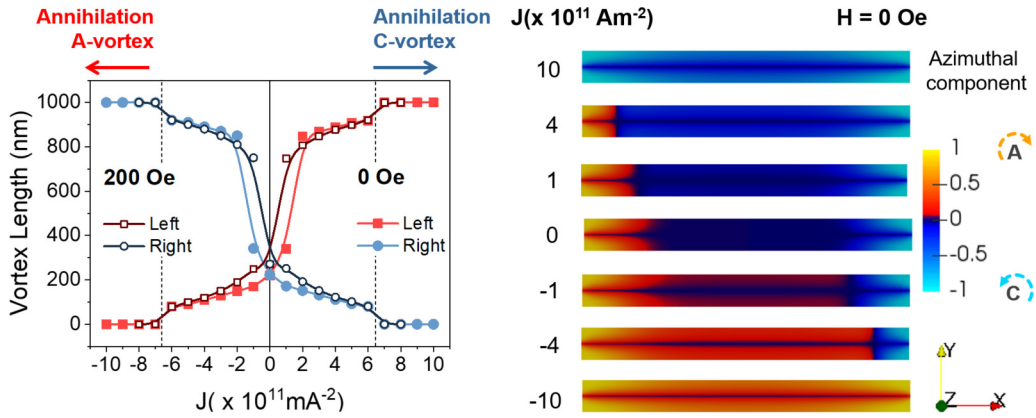

FIG. 2. Left: Length of each vortex domain at the left/right end of the nanowire measured from the ends of the nanowire as a function of applied current for zero and 200 Oe applied field. The lines are a guide for the eye. Right: Azimuthal component of the magnetization in the middle section of the nanowire for representative current densities and at zero applied field, where the yellow color corresponds to the clockwise rotation while the light blue color corresponds to the anticlockwise vorticity. The dark blue color corresponds to axial magnetization in the nanowire.

and current and the possibility of complete field-assisted switching under the Zhang-Li torque.

Figure 3(b) represents the diagram for the resulting stationary states where the yellow-shaded region denotes the situation where the magnetization core is not switched. One can clearly see the possibility to control the resulting vortex pattern (i.e., both nanowire core and shell) with fields and currents. Concerning the shell vorticity switching, the results are qualitatively the same as for zero applied field. However, the critical current for the rotational sense switching decreases as the field increases. Figure 2(a) also shows that the vortex length as a function of the current is practically independent on the applied field. Importantly, Fig. 3(a) indicates that the axial magnetization component can be switched with the assistance of the field and current and the critical field for switching decreases as a function of the applied current density, the switching process taking around 3 ns. It is worth noticing that the dynamics of the axial component of the magnetization is also independent of the current direction even under an applied magnetic field. Moreover, the analysis indicates that the magnetization curling along the nanowire (the vortex expansion due to the Oersted field) and the vorticity switching of the "incorrect" vortex occur prior to the switching of the axial (core) magnetization. The latter starts by the reversal of its axial component from the end of the nanowire where the vorticity was switched, towards the opposite end (see details of the dynamics in the Supplemental Material [38]). As reported earlier [22], we have observed that the magnetization switching in the nanowire core under an additional applied magnetic field is mediated by the propagation

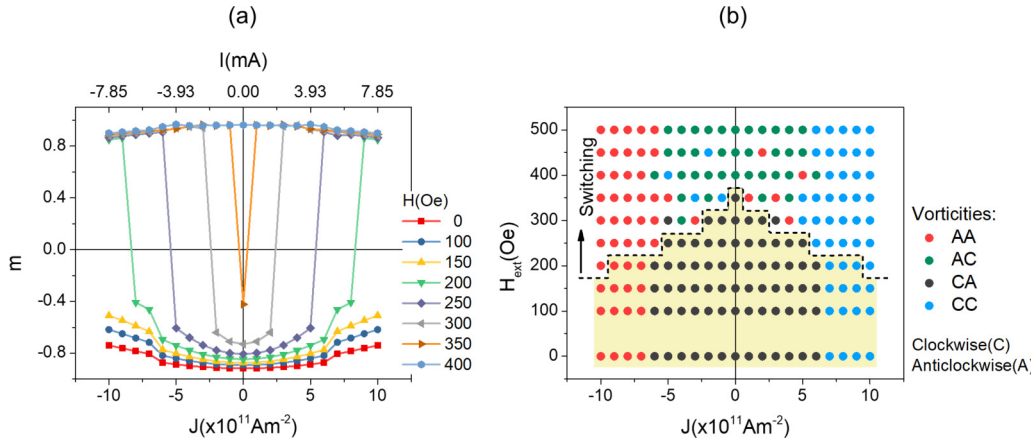

FIG. 3. (a) Axial magnetization of the final stationary state as a function of the current densities for various applied magnetic field values, indicating the threshold values for magnetization switching. On the top axis the equivalent electric current values are indicated for this nanowire. (b) Diagram of vortex states as a function of the applied field and current. Vorticity of the vortex (or curling) structures at the ends of the nanowire in the final magnetization state is indicated for different current densities and applied magnetic fields. C and A stand for Clockwise and Anticlockwise vorticity, in agreement with Figs. 1(b) and 2(b). The threshold for the axial component switching field is indicated by the dashed line and below this line (yellow-shaded region) no magnetization switching occurs. The chirality is determined by the product of the polarity and the vorticity.

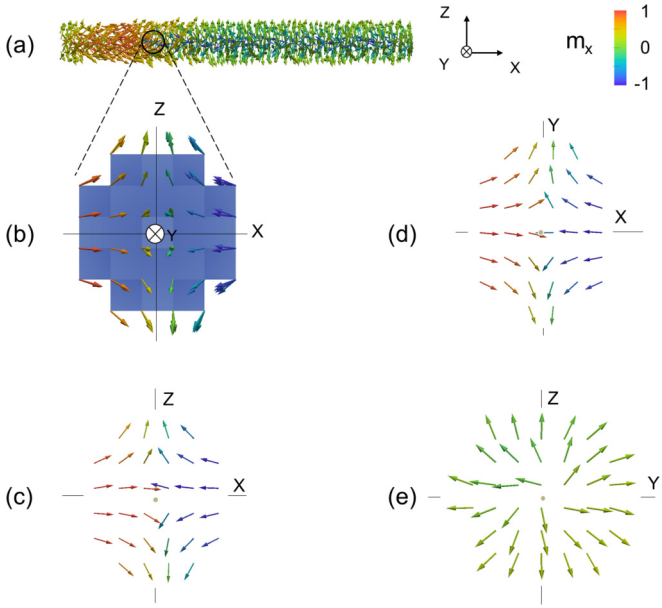

FIG. 4. Axial magnetization switching mediated by the Bloch point under current $6 \times 10^{11}\,\mathrm{A/m^2}$ and applied field 200 Oe. (a) The axial magnetization configuration at a certain time moment during the Bloch-point propagation. (b) A selected volume of size ∼8.5 nm centered at the area where the core of the vortex is reversing shows a Bloch-point singularity. (c)-(e) Magnetization at planes XZ, XY, and YZ of the structure in (b). Arrow colors indicate the value of the axial component of magnetization in every graph. The gray dots are guides for the eye showing where the Bloch point is located.

of the Bloch point (see Fig. 4). During this propagation the vorticity remains unchanged.

Regarding the curling structures in the steady state, the resulting vorticities, labeled as A (anticlockwise) and C (clockwise), have been collected in Fig. 3(b) as a function of the current density and the applied magnetic fields. For magnetic field values below the switching field (below the dashed line), the vorticities are determined by the current density as has been previously explained and can be controlled with adequate values of the magnetic field and current density. On the other hand, if the core magnetization switching takes place (above the dashed line), the rotation sense (vorticity) of both vortex structures is frequently reversed from CA to AC and vice versa for low current values. Since the Oersted field is not enough in this case to set the rotation senses, they are determined by the magnetization direction and the resulting torque and therefore a reversed pattern is found. Nevertheless, there are some low current values for which AA and CC are found when the magnetization is switched. This uncertainty is not observed for higher current values, for which the chirality is fully determined by the Oersted field, either AA or CC. The removal of the field and current do not change the vortex pattern and thus it can be completely controlled. It is worth noticing that below the dashed line (if there is no core magnetization switching) the chirality is completely determined by the vorticity, whereas above the dashed line the polarity is reversed, and the chirality is therefore determined by the polarity and the vorticity simultaneously. The switching of both polarity and vorticity preserves the chirality of the initial remanent state, whereas the switching of only the polarity or only the vorticity leads to chirality switching.

IV. CONCLUSIONS

In the present paper we have studied the dynamics of two domain walls naturally nucleated at the nanowire ends due to magnetostatic energy minimization. This can be considered as a needed step for the full control of wall motion in a vertical racetrack memory, based on cylindrical geometry. We have presented the state diagram for the vortex structure patterns (vorticity and polarity) in cylindrical Permalloy magnetic nanowires under an applied axial field and electric current. Our results indicate that in the absence of applied field the magnetization in the core stays parallel to the applied field direction. On the other hand, the current induces the expansion of the surface vortex domains, mainly via the Oersted field. The vortex structures at the end of the nanowire with the same (opposite) chirality as the Oersted field increase (decrease) their lengths. For higher current densities the vortex domain with the "good" chirality spans the entire nanowire length to the detriment of the vortex domain with "bad" chirality, which is finally annihilated at some critical current. Therefore, the vortex rotation sense (vorticity alone) can be set by the Oersted field produced by the current alone. In the presence of field, this happens prior to the change in polarity, i.e., nanowire core switching.

Consequently, the magnetic vortex pattern, i.e., the axial magnetization direction and the sense of rotation, can be set by an adequate application of axial magnetic field and currents with a suitable magnitude. The vorticity of the vortex structures can be controlled in the conditions of no magnetization switching. The magnetization (polarity) switching is only achieved by the application of a certain simultaneous magnetic minimum field (lower than the coercive field of the nanowire). Above the switching field, the chiralities of the vortex structures in the final state can be mostly predicted for low values of the current density and controlled for high currents, for which the vorticity is determined by the Oersted field. In this regime the switching does not change the vorticity pattern.

The control of the chiralities and the expansion of the vortex structures from the end are thus concluded to become quite relevant for future information technologies based on 3D vertical structures. For these applications, a controlled nucleation and pinning of domain walls is necessary. In this concern, in cylindrical nanowires the switching could be controlled in addition by appropriate geometry and/or compositional modulations as has been probed in Refs. [4,23,36,40]. Our state diagram will be very useful for future experimental realizations of current-induced domain wall dynamics in cylindrical magnetic nanowires.

ACKNOWLEDGMENT

The authors are thankful for the support from Spanish Ministry of Economy and Competitiveness (MINECO) under Project MAT2016-76824-C3-1-R and from the Regional Government of Madrid under Project S2018/NMT-4321 NANOMAGCOST-CM.

[1] S. Parkin and S.-H. Yang, Nat. Nanotechnol. **10**, 195 (2015).

[2] F. Nasirpouri, S. M. Peighambari-Sattari, C. Bran, E. M. Palmero, E. Berganza Eguiarte, M. Vazquez, A. Patsopoulos, and D. Kechrakos, Sci. Rep. **9**, 9010 (2019).

[3] S. Ruiz-Gómez, M. Foerster, L. Aballe, M. P. Proenca, I. Lucas, J. L. Prieto, A. Mascaraque, J. de la Figuera, A. Quesada, and L. Pérez, Sci. Rep. **8**, 16695 (2018).

[4] C. Bran, E. Berganza, J. A. Fernandez-Roldan, E. M. Palmero, J. Meier, E. Calle, M. Jaafar, M. Foerster, L. Aballe, A. Fraile Rodriguez, R. P. del Real, A. Asenjo, O. Chubykalo-Fesenko, and M. Vazquez, ACS Nano **12**, 5932 (2018).

[5] J. Garcia, V. M. Prida, V. Vega, W. O. Rosa, R. Caballero-Flores, L. Iglesias, and B. Hernando, J. Magn. Magn. Mater. **383**, 88 (2015).

[6] A. Moskaltsova, M. P. Proenca, S. V. Nedukh, C. T. Sousa, A. Vakula, G. N. Kakazei, S. I. Tarapov, and J. P. Araujo, J. Magn. Magn. Mater. **374**, 663 (2015).

[7] E. D. Barriga-Castro, J. García, R. Mendoza-Reséndez, V. M. Prida, and C. Luna, RSC Adv. **7**, 13817 (2017).

[8] J. García, V. M. Prida, L. G. Vivas, B. Hernando, E. D. Barriga-Castro, R. Mendoza-Reséndez, C. Luna, J. Escrig, and M. Vázquez, J. Mater. Chem. C **3**, 4688 (2015).

[9] V. Raposo, M. Zazo, A. G. Flores, J. Garcia, V. Vega, J. Iñiguez, and V. M. Prida, J. Appl. Phys. **119**, 143903 (2016).

[10] Y. P. Ivanov, M. Vázquez, and O. Chubykalo-Fesenko, J. Phys. D: Appl. Phys. **46**, 485001 (2013).

[11] C. Bran, E. Berganza, E. M. Palmero, J. A. Fernandez-Roldan, R. P. del Real, L. Aballe, M. Foerster, A. Asenjo, A. Fraile Rodríguez, and M. Vazquez, J. Mater. Chem. C **4**, 978 (2016).

[12] C. Bran, J. A. Fernandez-Roldan, E. M. Palmero, E. Berganza, J. Guzman, R. P. del Real, A. Asenjo, A. Fraile Rodríguez, M. Foerster, L. Aballe, O. Chubykalo-Fesenko, and M. Vazquez, Phys. Rev. B **96**, 125415 (2017).

[13] R. Wieser, U. Nowak, and K. D. Usadel, Phys. Rev. B **69**, 064401 (2004).

[14] C. A. Ferguson, D. A. MacLaren, and S. McVitie, J. Magn. Magn. Mater. **381**, 457 (2015).

[15] M. Staňo and O. Fruchart, *Magnetic wires and nanotubes, in Handbook of Magnetic Materials*, edited by E. Bruck, Vol. 27 (North-Holland, Amsterdam, 2018), Chap. 3, pp. 155–267.

[16] R. Hertel, J. Phys. Condens. Matter **28**, 483002 (2016).

[17] S. Da Col, S. Jamet, N. Rougemaille, A. Locatelli, T. O. Mentes, B. S. Burgos, R. Afid, M. Darques, L. Cagnon, J. C. Toussaint, and O. Fruchart, Phys. Rev. B **89**, 180405(R) (2014).

[18] H. Forster, T. Schrefl, D. Suess, W. Scholz, V. Tsiantos, R. Dittrich, and J. Fidler, J. Appl. Phys. **91**, 6914 (2002).

[19] A. Wartelle, B. Trapp, M. Stano, C. Thirion, S. Bochmann, J. Bachmann, M. Foerster, L. Aballe, T. O. Mentes, A. Locatelli, A. Sala, L. Cagnon, J.-C. Toussaint, and O. Fruchart, Phys. Rev. B **99**, 024433 (2019).

[20] E. Feldtkeller, Z. Angew. Phys. **19**, 530 (1965) [IEEE. Trans. Magn. **53**, 0700308 (2017).

[21] W. Döring, J. Appl. Phys. **39**, 1006 (1968).

[22] M. Charilaou, H.-B. Braun, and J. F. Löffler, Phys. Rev. Lett. **121**, 097202 (2018).

[23] J. A. Fernandez-Roldan, R. Perez del Real, C. Bran, M. Vazquez, and O. Chubykalo-Fesenko, Nanoscale **10**, 5923 (2018).

[24] J. A. Fernandez-Roldan, Yu. P. Ivanov, and O. Chubykalo-Fesenko, in *Magnetic Nano- and Microwires (2nd edition)*, edited by M. Vazquez (Elsevier, Amsterdam, 2020), Chap. 14, pp. 403–426.

[25] R. Hertel, SPIN **03**, 1340009 (2013).

[26] M. Yan, C. Andreas, A. Kákay, F. García-Sánchez, and R. Hertel, Appl. Phys. Lett. **100**, 252401 (2012).

[27] M. Staňo, S. Jamet, J. C. Toussaint, S. Bochmann, J. Bachmann, A. Masseboeuf, C. Gatel, and O. Fruchart, J. Phys.: Conf. Ser. **903**, 012055 (2017).

[28] L. A. Rodríguez, C. Bran, D. Reyes, E. Berganza, M. Vázquez, C. Gatel, E. Snoeck, and A. Asenjo, ACS Nano **10**, 9669 (2016).

[29] F. Abreu Araujo, L. Piraux, V. A. Antohe, V. Cros, and L. Gence, Appl. Phys. Lett. **102**, 222402 (2013).

[30] F. Abreu Araujo, M. Darques, K. A. Zvezdin, A. V. Khvalkovskiy, N. Locatelli, K. Bouzehouane, V. Cros, and L. Piraux, Phys. Rev. B **86**, 064424 (2012).

[31] M. Darques, A. Dussaux, A. v. Khvalkovskiy, J. de la Torre Medina, F. Abreu Araujo, R. Guillemet, K. Bouzehouane, S. Fusil, J. Grollier, G. G. Avanesyan, K. A. Zvezdin, V. Cros, and L. Piraux, J. Phys. D: Appl. Phys. **44**, 105003 (2011).

[32] M. Schobitz, A. De Riz, S. Martin, S. Bochmann, C. Thirion, J. Vogel, M. Foerster, L. Aballe, T. O. Mentes, A. Locatelli, F. Genuzio, S. Le-Denmat, L. Cagnon, J. C. Toussaint, D. Gusakova, J. Bachmann, and O. Fruchart, Phys. Rev. Lett. **123**, 217201 (2019).

[33] M. P. Proenca, M. Muñoz, I. Villaverde, A. Migliorini, V. Raposo, L. Lopez-Diaz, E. Martinez, and J. L. Prieto, Sci. Rep. **9**, 17339 (2019).

[34] A. Thiaville and Y. Nakatani, in *Nanomagnetism and Spintronics* (Elsevier, Amsterdam, 2014), pp. 261–313.

[35] D. Castilla, M. Maicas, J. L. Prieto, and M. P. Proenca, J. Phys. D: Appl. Phys. **50**, 105001 (2017).

[36] A. de Riz, B. Trapp, J. A. Fernandez-Roldan, Ch. Thirion, J.-Ch. Toussaint, O. Fruchart, and D. Gusakova, in *Magnetic Nano- and Microwires (2nd edition)*, edited by M. Vazquez (Elsevier, Amsterdam, 2020), Chap. 15, pp. 427–453.

[37] A. Vansteenkiste and B. van de Wiele, J. Magn. Magn. Mater. **323**, 2585 (2011).

[38] See Supplemental Material at http://link.aps.org/supplemental/10.1103/PhysRevB.102.024421 for further details.

[39] S. Zhang and Z. Li, Phys. Rev. Lett. **93**, 127204 (2004).

[40] J. A. Fernandez-Roldan, A. de Riz, B. Trapp, C. Thirion, M. Vazquez, J. C. Toussaint, O. Fruchart, and D. Gusakova, Sci. Rep. **9**, 5130 (2019).